DOI: 10.1002/chem.201001929

Cation–Cation Complexes of Pentavalent Uranyl: From Disproportionation Intermediates to Stable Clusters

Victor Mougel, Pawel Horeglad, Grégory Nocton, Jacques Pécaut, and Marinella Mazzanti*[a]

Abstract: Three new cation–cation complexes of pentavalent uranyl, stable with respect to the disproportionation reaction, have been prepared from the reaction of the precursor $[(UO_2py_5)(KI_2py_2)]_n$ (**1**) with the Schiff base ligands salen^{2-}, acacen^{2-}, and salophen^{2-} (H_2salen = *N*,*N*′-ethylene-bis(salicylideneimine), H_2acacen = *N*,*N*′-ethylene-bis(acetylacetoneimine), H_2salophen = *N*,*N*′-phenylene-bis(salicylideneimine)). The preparation of stable complexes requires a careful choice of counter ions and reaction conditions. Notably the reaction of **1** with salophen^{2-} in pyridine leads to immediate disproportionation, but in the presence of [18]crown-6 ([18]C-6) a stable complex forms. The solid-state structure of the four tetranuclear complexes, $\{[UO_2(acacen)]_4[\mu_8\text{-}]_2[K([18]C\text{-}6)(py)]_2\}$ (**3**) and $\{[UO_2(acacen)]_4[\mu_8\text{-}]\}\cdot 2[K([222])(py)]$ (**4**), $\{[UO_2(salophen)]_4[\mu_8\text{-}K]_2[\mu_5\text{-}KI]_2[(K([18]C\text{-}6)]\}\cdot 2[K([18]C\text{-}6)(thf)_2]\cdot 2I$ (**5**), and $\{[UO_2(salen)_4][\mu_8\text{-}Rb]_2[Rb([18]C\text{-}6)]_2\}$ (**9**) ([222] = [222]cryptand, py = pyridine), presenting a T-shaped cation–cation interaction has been determined by X-ray crystallographic studies. NMR spectroscopic and UV/Vis studies show that the tetranuclear structure is maintained in pyridine solution for the salen and acacen complexes. Stable mononuclear complexes of pentavalent uranyl are also obtained by reduction of the hexavalent uranyl Schiff base complexes with cobaltocene in pyridine in the absence of coordinating cations. The reactivity of the complex $[U^VO_2(salen)(py)][Cp^*_2Co]$ with different alkali ions demonstrates the crucial effect of coordinating cations on the stability of cation–cation complexes. The nature of the cation plays a key role in the preparation of stable cation–cation complexes. Stable tetranuclear complexes form in the presence of K^+ and Rb^+, whereas Li^+ leads to disproportionation. A new uranyl–oxo cluster was isolated from this reaction. The reaction of $[U^VO_2(salen)(py)][Cp^*_2Co]$ (Cp* = pentamethylcyclopentadienyl) with its U^{VI} analogue yields the oxo-functionalized dimer $[UO_2(salen)(py)]_2[Cp^*_2Co]$ (**8**). The reaction of the $\{[UO_2(salen)_4][\mu_8\text{-}K]_2[K([18]C\text{-}6)]_2\}$ tetramer with protons leads to disproportionation to U^{IV} and U^{VI} species and H_2O confirming the crucial role of the proton in the U^V disproportionation.

Keywords: actinides · cluster compounds · disproportionation · Schiff bases · uranium

Introduction

The chemistry of pentavalent uranyl and its role as an intermediate species in uranium redox reactivity are relevant in the nuclear industry and for environmental concerns associated with potential uranium release during the long-term storage of spent nuclear fuel.[1–8] Unlike uraniums radioactive neighbors, NpO_2^+ and PuO_2^+, which are stable under a wide range of conditions, pentavalent uranyl can be stabilized in concentrated carbonate media[9–11] or in reducing environments at mineral surfaces,[2] but otherwise it readily disproportionates in water to U^{IV} and uranyl(VI) species.[1] Some recent advances on the isolation of this species in non-aqueous and anaerobic conditions have been the focus of several reviews.[12–14] However, because of its low stability only limited information is available on the reactivity and physicochemical properties of molecular pentavalent uranyl complexes relative to other uranium species.[15–17] Kinetic and theoretical studies suggest that the disproportionation reaction involves the formation of a dimeric cation–cation complex presenting two mutually coordinated UO_2^+ groups,

[a] V. Mougel, Dr. P. Horeglad, Dr. G. Nocton, Dr. J. Pécaut, Dr. M. Mazzanti
CEA, INAC, SCIB, Laboratoire de Reconnaissance Ionique et Chimie de Coordination, CEA-Grenoble
38054 GRENOBLE, Cedex 09 (France)
Fax: (+33) 438 785 090
E-mail: marinella.mazzanti@cea.fr

Supporting information for this article is available on the WWW under http://dx.doi.org/10.1002/chem.201001929.

which is followed by the protonation of the uranyl oxygen atoms to yield UO_2^{2+} and U^{4+} species.[8,18,19] Therefore, the exclusion of protons by using nonaqueous solvents and the use of a bulky ligand to prevent cation–cation interactions have been considered as essential steps for the preparation of stable pentavalent uranyl complexes .[20,21] Notably, Ikeda and co-workers have provided spectroscopic evidence that uranyl(V) compounds can be electrochemically produced from the reduction of uranyl(VI) in the presence of ligands of various denticicity (mono, bi-, tetra-, or pentadentate), such as diketonates and Schiff bases, by using the aprotic solvent DMSO.[22–26] Stable complexes of pentavalent uranyl were shown to form in aprotic media in the presence of appropriate sets of ligands. In these systems, DMSO acts as a ligand competing with the uranyl oxygen atom for the coordination of the uranium center and, therefore, prevents cation–cation interactions even in the absence of bulky ligands.[27] Recently, we have shown that tetranuclear and dinuclear cation–cation complexes can be isolated depending on the used conditions from the reaction of the useful U^V precursor $[(UO_2py_5)(KI_2py_2)]_n$ (**1**; py = pyridine)[28] with dibenzoylmethanate (dbm^-) in pyridine.[27,29] These compounds have limited solution stability and undergo disproportionation to form UO_2^{2+} and U^{4+} species pointing to the important role of cation–cation intermediates in the disproportionation mechanism.[27,29] To prevent the formation of polynuclear intermediates leading to disproportionation ours and other groups have designed bulky polydentate ligands or macrocyclic ligands that have resulted in the preparation of stable complexes of pentavalent uranyl.[21,31–34]

These initial results seemed to validate the general assumption that the formation of cation–cation complexes would inevitably result in the disproportionation of the pentavalent uranyl species.

However, in contrast with this general belief, very recently we have provided unambiguous evidence that stable polynuclear cation–cation complexes of pentavalent uranyl can be prepared in the presence of a tetradentate Schiff base ligand. The stable UO_2^+–UO_2^+ cation–cation $\{[UO_2(salen)]_4[\mu_8\text{-}K]_2\}\cdot 2[K([18]C\text{-}6)(py)]$ (**2**) ([18]C-6 = [18]crown-6) complex can be prepared from the reaction of $[(UO_2py_5)(KI_2py_2)]_n$ (**1**) with the Schiff base ligand $salen^{2-}$ (H_2salen = *N*,*N*′-ethylene-bis(salicylideneimine)).[35] Complex **2** is stable with respect to the disproportionation reaction even in the presence of stoichiometric amounts of water, but can be easily oxidized to yield a $3U^V/1U^{VI}$ species providing a route to mixed-valent assemblies.[35]

Cation–cation interactions are an important structural feature in the chemistry of neptunyl(V) and plutonyl(V)[36–43], which is likely to be responsible for the formation of insoluble aggregates and complex mixtures in nuclear waste, resulting in technological problems in the reprocessing and storage of nuclear waste.[1,44] The anticipated role of cation–cation complexes as intermediates in the disproportionation of pentavalent uranyl seemed to rule out the possibility of developing such chemistry for U^V. Our preliminary report of a stable cation–cation complex of pentavalent uranyl suggests that such polymetallic species can be stabilized by an appropriate choice of conditions and ligands. As a result, cation–cation interactions could become a convenient route to the expansion of uranium supramolecular chemistry.[45–47] With the aim of gaining some insight on the parameters leading to stable cation–cation complexes versus disproportionation products, we have now investigated the reaction of pentavalent uranyl with different Schiff base ligands possessing different geometric and electronic properties and in the presence of different alkali ions. We report the synthesis of two new tetrameric cation–cation complexes of pentavalent uranyl with the $acacen^{2-}$ ($H_2acacen$ = *N*,*N*′-ethylene-bis(acetylacetoneimine)) and the $salophen^{2-}$ ($H_2salophen$ = *N*,*N*′-phenylene-bis(salicylideneimine)) ligands and their reactivity. We show here that the nature of the alkali ion has an important effect on the stability of the cation–cation complex with respect to the disproportionation reaction.

Results and Discussion

Synthesis and solution structure: Three tetranuclear complexes of pentavalent uranyl were prepared by using the Schiff base ligands $salen^{2-}$, $acacen^{2-}$, and $salophen^{2-}$, which have different geometric and electronic characteristics. The stable tetrameric complex $\{[UO_2(salen)]_4[\mu_8\text{-}K]_2\}\cdot 2[K([18]C\text{-}6)(py)]$ (**2**) was prepared in 70% yield as previously reported[35] from the reaction of the uranyl(V) precursor **1** with one equivalent of $salenK_2$ in the presence of [18]crown-6 ether in pyridine. We have previously reported that the reaction of **1** with $salenK_2$ in the absence of [18]C-6 yields[35] an insoluble compound of formula $[UO_2(salen)K(py)]\cdot 1.4\,KI$, probably of polymeric structure, which can be dissolved in pyridine solutions containing [18]C-6 to afford **2**. ^1H NMR spectroscopic studies in deuterated pyridine show that the reaction of **1** with the Schiff base salt $acacenK_2$ yields a uranyl(V) compound that is stable for more than 30 days under an argon atmosphere. Isolation of this compound in a pure form proved difficult because of its high solubility in pyridine. However the tetrameric pentavalent uranyl complexes $\{[UO_2(acacen)]_4[\mu_8\text{-}K]_2[K([18]C\text{-}6)(py)]_2\}$ (**3**) and $\{[UO_2(acacen)]_4[\mu_8\text{-}K]\}\cdot 2[K([222])(py)]$ (**4**) ([222] = [222]cryptand) can be prepared in analytically pure in 34 and 53% yields[48] from the reaction of **1** with $acacenK_2$ in pyridine, followed by addition of [18]C-6 or of [222]cryptand, respectively (Scheme 1). X-ray quality crystals of **3** and **4** were obtained by slow diffusion of iPr_2O into the resulting pyridine solution. ^1H NMR spectroscopic studies in pyridine show that **3** and **4** are stable with respect to the disproportionation reaction over 30 days.

Pulsed-field gradient stimulated echo (PFGSTE) diffusion NMR spectroscopy[49] was used to measure the diffusion coefficient (D) of **4** in 1 mM pyridine solutions by using the U^{VI} complex $[UO_2(salophen)(py)]$[50] as an external reference. Since the diffusion coefficient is a function of the molecular weight, the Stokes–Einstein equation can be used to estimate the relative molecular size of the solution species

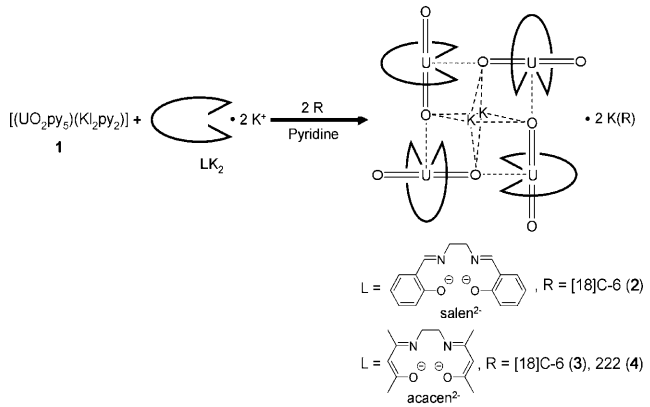

Scheme 1. Reaction of **1** with K_2salen and K_2acacen to yield **2** and **4**.

(see the Supporting Information for details).[51] The D value measured for **4** ($D = 2.94(6) \times 10^{-10}\ m^2 s^{-1}$ in pyridine) suggests the presence of a tetrameric species in pyridine and acetonitrile solution similar to what was already found for **2**[35] and for the dibenzoylmethanate (dbm^-) tetramer $[UO_2(dbm)_2]_2[\mu\text{-}K(py)_2]_2[\mu_8\text{-}K(py)]_2I_2{\cdot}py_2$.[27,29] ESI-MS studies also point to the presence of a tetramer in pyridine solution (m/z: 1023.2, corresponding to $[UO_2(acacen)]_2[\mu_8\text{-}K]_2^{2-}$; see Figure S1 in the Supporting Information). These results show that the coordination properties of the $acacen^{2-}$ ligand are very similar to those of $salen^{2-}$ in the reaction with the pentavalent uranyl iodide **1**. Moreover, the final tetrameric complex is stable with respect to the disproportionation reaction, which is similar to what was found for the salen tetramer.[35] In contrast, the reaction of the fully aromatic analogue of the $salen^{2-}$ ligand $salophen^{2-}$ with the uranyl(V) polymer **1** in pyridine has a very different outcome. ^{1}H NMR spectroscopic studies show that this reaction leads rapidly to the formation of a complicated mixture of disproportionation products (see Figure S2 in the Supporting Information). We were able to identify the presence of the NMR spectroscopic signals arising from the previously reported U^{VI} and U^{IV} complexes $[UO_2(salophen)(py)]$ and $[U(salophen)_2]$, which were independently prepared.[24,52] Several other decomposition products remain unidentified. To understand the origin of the different stability observed for these similar ligand systems and to assess the role of potassium in the disproportionation mechanism [18]C-6 was added to the $salophenK_2$ solution before reacting it with **1**, which resulted in a very different behavior (see Figure S3 in the Supporting Information). Notably the diffusion of iPr_2O into the resulting green pyridine solution produces a powder that after recrystallization from THF yields the tetrameric complex $\{[UO_2(salophen)]_4[\mu_8\text{-}K]_2[\mu_5\text{-}KI]_2[(K([18]C\text{-}6)]\}{\cdot}2[K([18]C\text{-}6)(thf)_2]{\cdot}2I$ (**5**) in a moderate yield. This complex shows a structure similar to that found for the salen and acacen tetramers presenting four uranyl moieties linked with the same T-shaped cation–cation interaction to form a square core as shown in Scheme 2. A pyridine solution of **5** is stable towards disproportionation for up to 30 days in pyridine. It is interesting to notice that the addition of a catalytic excess of KI with respect to [18]C-6 (0.1 equivalents) in pyridine is sufficient to promote the complete disproportionation of **5** in two days.

PGFSTE diffusion NMR spectroscopic studies were performed to investigate the nuclearity of complex **5** in pyridine. The measured hydrodynamic radius of **5** ($D = 5.40(1) \times 10^{-10}$, $r_{sph} = 4.6$ Å) suggests the presence of mononuclear species in pyridine. This behavior differs from what was observed for the acacen and salen complexes **2**, **3**, and **4**, which retain their tetrameric structure in both pyridine and DMSO.[35] The stability of **5** in pyridine is probably associated with its monomeric form while, in the absence of crown ether, the presence of the potassium ion leads to the formation of a reactive tetrameric species. Similar to what was previously reported for the UO_2^+ complex of the bulky salophen-tBu_2 ligand[21] ^{1}H NMR spectroscopic studies show that the reduction of the U^{VI} complex $[UO_2(salophen)(py)]$ with Cp^*_2Co ($Cp^* =$ pentamethylcyclopentadienyl) in pyridine affords the stable complex of pentavalent uranyl $[UO_2(salophen)(py)][Cp^*_2Co]$ (**6**) (see Figure S4 in the Support-

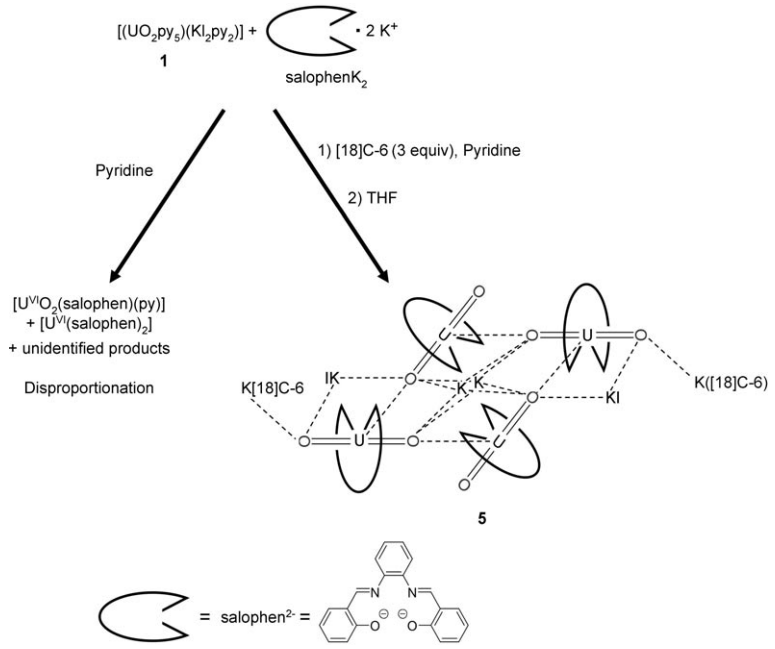

Scheme 2. The reaction of **1** with K_2salophen in the presence or absence of [18]C-6 leads to the stabilization of U^V to yield **5** or to the disproportionation, respectively.

ing Information) The isolation of this complex in the solid state proved difficult due to its tendency to disproportionate in the presence of cosolvents, such as *n*-hexane, or in other solvent combinations. Addition of KI to a pyridine solution of **6** results in rapid disproportionation, whereas the addition of K([18]C-6)I yields complex **5**. In the UO_2^+ complex of the salophen-tBu_2 ligand,[21] the bulky substituents of the Schiff base ligand offer sterical protection to the uranyl(V) moiety preventing cation–cation interactions that result in a high stability. The results presented here show that tetradentate Schiff base ligands can stabilize pentavalent uranyl in pyridine by preventing cation–cation interactions even in the absence of bulky substituents on the Schiff base ligand if the reaction conditions are suitably chosen. In particular, in the absence of a strong coordinating cation, the pyridine provides a competitive ligand with respect to the uranyl oxygen atom of another pentavalent complex. Stability with respect to disproportionation had been previously observed for $[U^VO_2(salophen)(dmso)]^-$ in the absence[23] and presence[27] of coordinating cations because of the stronger affinity of the DMSO ligand for the uranium(V) center. In solvents less coordinating than DMSO and in the presence of coordinating cations, the complex of uranyl(V) with salophen forms a tetranuclear cation–cation complex, which leads eventually to disproportionation. This contrasts with the behavior of the tetramers formed with salen and acacen, which are fully stable towards disproportionation. However, a suitable choice of the reaction conditions renders it possible to prepare a stable cation–cation complex also for the salophen ligand.

The solution structure and stability of these tetrameric complexes has also been investigated by visible-near IR spectroscopy. The Vis-NIR spectra of the complexes of pentavalent uranyl described in this work show different bands depending on their nuclearity in solution. The cation–cation complexes **4**, **2**, and the previously reported $[UO_2(dbm)_2]_2$-$[\mu$-$K(py)_2]_2[\mu_8$-$K(py)]\cdot 2I_2\cdot py_2$ complex,[27] which retain their tetranuclear structure in pyridine, show in pyridine solution a well-resolved band at around 960 nm, with a moderate absorption coefficient ($\varepsilon = 200\,L\,mol^{-1}\,cm^{-1}$) (Figure 1). The same feature was also previously observed for **2** in DMSO for which this complex was found by NMR spectroscopic studies to retain its tetrameric structure (see Table S1 in the Supporting Information).[35] In contrast, the Vis-NIR spectrum of mononuclear complexes of pentavalent uranyl with Schiff bases is significantly different showing a large poorly resolved band in the region of 800–1000 nm with a $200\,L\,mol^{-1}\,cm^{-1}$ absorption coefficient. Such types of absorption spectrum have been observed for the mononuclear complex $[UO_2(salophen\text{-}tBu_2)(py)K]$[21] in pyridine and for the monomeric complexes $[UO_2(salophen)(dmso)]^-$, $[UO_2(dbm)_2(dmso)]^-$, and $[UO_2(saldien)]^-$ in DMSO.[20,23] A similar spectrum is also measured for **5** in pyridine solution (see Figure S5 in the Supporting Information) for which the complex was found to be monomeric by ^1H NMR spectroscopic experiments. The spectral differences observed between polynuclear and mononuclear complexes could arise from the difference in symmetry between the two types of structure affecting the f–f transition and should prove useful for detecting the presence of cation–cation assemblies in solution. Variations in the Vis-NIR spectrum associated to the formation of cation–cation complexes have been previously observed for neptunyl(V) compounds.[36] The addition of one to two equivalents of KI to a pyridine solution of **5** leads to a change in the shape of the spectrum yielding a spectrum featuring the characteristic band at 950 nm (see the green curve in Figure S5 in the Supporting Information). If excess [18]C-6 is again added to this solution the broad original spectrum is restored showing the reversibility of this reaction. The UV/Vis spectrum of **5** measured in THF solution also shows the band at 950 nm in agreement with the presence of a tetranuclear structure. The Vis-NIR results are in agreement with the ^1H NMR spectroscopic experiments and suggest that the complex **5** dissociates in pyridine, whereas the addition of K^+ favors the formation of a reactive cation–cation complex, which results in the disproportionation of the pentavalent uranyl complex. The stability of **5** in THF, which is present as a tetrameric complex, can be associated to the replacement of the K^+ ion with the $K([18]C\text{-}6)^+$ ion. This suggests that the cationic nature affects significantly the stability of cation–cation complexes and further results in this direction are presented in the reactivity section.

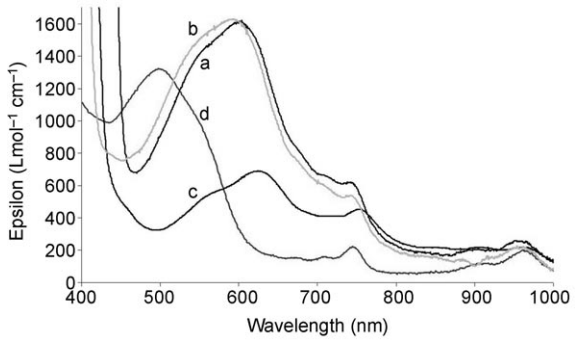

Figure 1. UV/Vis spectra of **2** in pyridine (a), of **2** in DMSO (b), of $\{[UO_2(dbm)_2]_2[\mu$-$K(py)_2]_2[\mu_8$-$K(py)]\}_2I_2\cdot py_2$ (c), and of **4** in pyridine (d).

Solid-state structure: The crystal structure of complex **2** has been described in a previous report.[35] The crystal structures of complexes **3**, **4**, and **5** were determined by single-crystal X-ray diffraction. The structures of **3** and **4** and of the tetrameric cores in complexes **2**, **3**, and **4** are presented in Figure 2, whereas the structure of **5** and its tetrameric core are presented in Figure 3. Selected bond lengths and angles for these complexes are presented in Table 1. The structures of **2**, **3**, **4**, and **5** all consist of a centrosymmetric tetramer of UO_2^+ cations coordinated to each other in a monodentate fashion to form a square plane with two crystallographically nonequivalent uranyl complexes. In the structure of **3**, **4**, and **5**, two symmetry related potassium ions are found above and below the plane of the UO_2^+ tetrameric core (at 2.08 (in **3**), 2.13 (in **4**), and 2.28 Å (in **5**)), respectively. Both

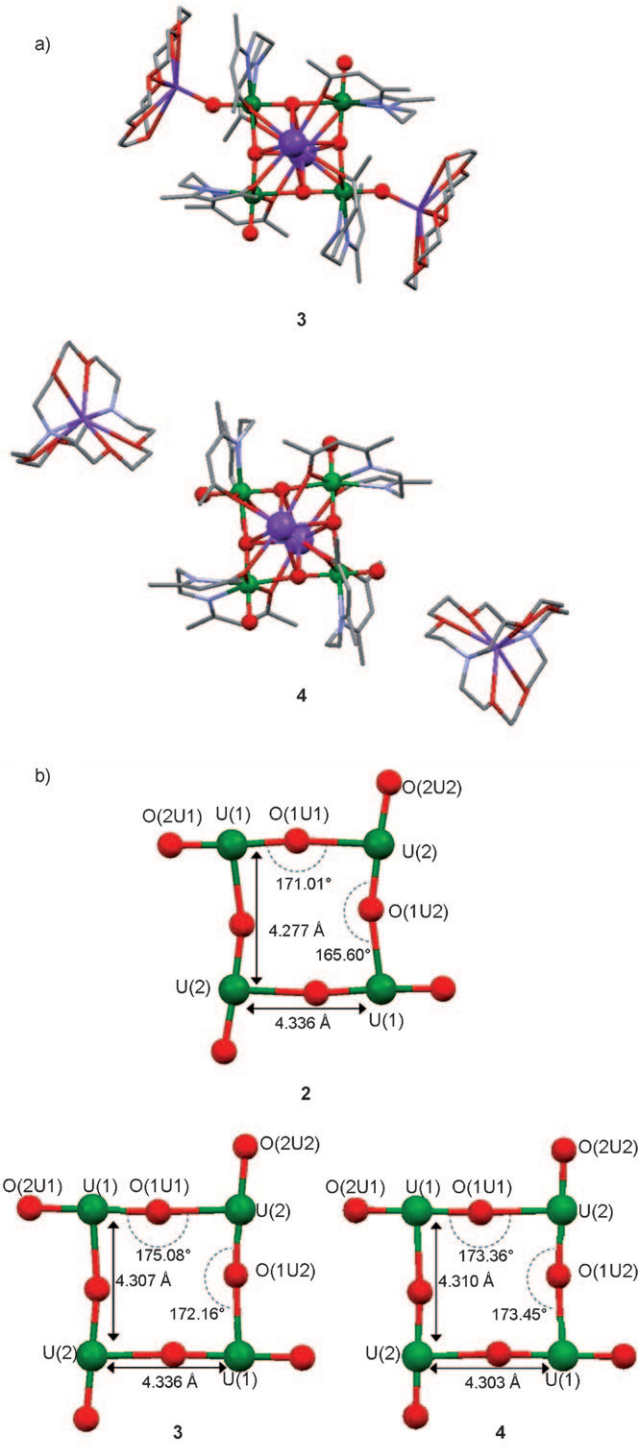

Figure 2. a) Mercury diagrams of the complexes **3** and **4**. b) Metric comparison between the tetrameric core of complexes **2**, **3**, and **4**, showing the interacting UO_2^+/UO_2^+ with associated distances and angles. The structures are represented along the axis formed by the two potassium ions and perpendicular to the plane of the uranium atoms (H atoms were omitted for clarity, C are represented in grey, O in red, K in purple, N in blue, and U in green).

potassium ions coordinate four different uranyl oxygen atoms and four different ligand oxygen atoms. It is remarkable that in the presence of [18]C-6 or [222]cryptand even in excess, the potassium binds preferentially to the uranyl oxygen atoms rather than to [18]C-6 or [222]cryptand. A similar potassium coordination mode (at 2.14 Å above and below the plane) was found in complex **2**. In **4**, as previously found for **2**, there are the only two central potassium ions forming a cation–cation interaction with the uranyl oxygen

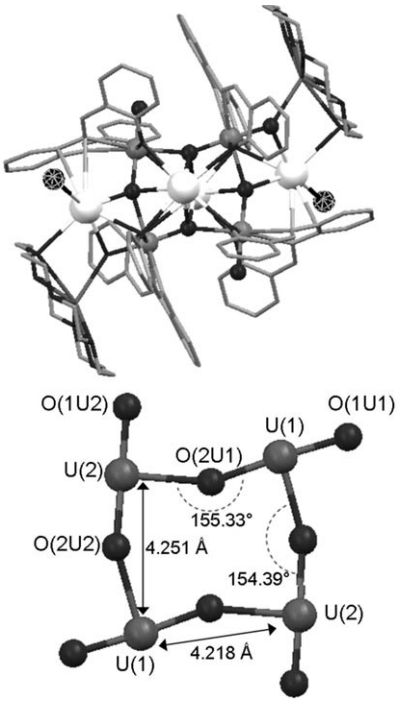

Figure 3. Mercury view and core detailed of complex **5** with associated distances and angles. The structures are represented along the axis formed by the two potassium ions perpendicular to the plane of the uranium atoms (ligands are represented with grey pipes, O in black, K in white, I in black with white stripes, and U in grey.).

Table 1. Selected bond lengths [Å] and angles [°] in complexes **2**–**5** and **9**.

Bond lengths [Å]	**2**	**3**	**4**	**5**	**9**
U(1)–O(1U1)	1.936(5)	1.937(11)	1.912(11)	1.942(3)	1.928(9)
U(1)–O(2U1)	1.841(5)	1.853(12)	1.768(11)	1.871(4)	1.836(10)
U(1)–O(1U2)	2.421(5)	2.344(9)	2.373(9)	2.404(3)	2.414(9)
U(1)–O(1)	2.358(6)	2.366(13)	2.373(9)	2.295(3)	2.356(11)
U(1)–O(2)	2.342(6)	2.341(12)	2.374(9)	2.346(3)	2.321(11)
U(1)–N(1)	2.671(7)	2.629(15)	2.401(10)	2.598(4)	2.614(11)
U(1)–N(2)	2.594(7)	2.572(15)	2.558(10)	2.666(4)	2.625(7)
U(2)–O(1U2)	1.929(5)	1.973(9)	1.909(10)	1.954(3)	1.909(9)
U(2)–O(2U2)	1.840(5)	1.858(11)	1.799(9)	1.818(3)	1.882(8)
U(2)–O(2U1)	2.374(5)	2.403(11)	2.375(9)	2.374(3)	2.419(9)
U(2)–O(21)	2.348(6)	2.372(12)	2.375(9)	2.365(3)	2.351(12)
U(2)–O(22)	2.386(6)	2.367(13)	2.405(11)	2.370(3)	2.334(11)
U(2)–N(21)	2.630(7)	2.542(16)	2.408(11)	2.617(4)	2.721(12)
U(2)–N(22)	2.631(6)	2.444(15)	2.550(13)	2.660(4)	2.625(14)
Angles [°]	**2**	**3**	**4**	**5**	**9**
O(1U1)-U(1)-O-(2U1)	176.9(2)	177.4(5)	179.3(4)	175.37(14)	175.3(3)
O(2U2)-U(2)-O-(1U2)	176.2(2)	179.3(5)	179.2(4)	174.72(15)	177.1(5)
U(1)-O(1U1)-U(2)	171.0(3)	175.0(7)	173.4(5)	154.39(18)	171.2(6)
U(2)-O(1U2)-U(1)#1	165.6(3)	172.2(6)	173.4(4)	155.33(16)	171.2(4)

atoms, whereas the two remaining potassium counterions are found as isolated $(([18]C\text{-}6)K)^+$ and $([222]K)^+$ ions in the unit cells of **2** and **4**, respectively). In **3** and **5** the bulky $(([18]C\text{-}6)K)^+$ ions are involved in a cation–cation interaction with two different uranyl oxygen atoms located at the opposite sides of the tetramer. Moreover, in **5** two additional potassium ions are located on opposite sides of the tetranuclear complex bridging uranyl oxygen atoms from two different uranyl groups. The charge of these two symmetry related potassium ions is balanced by a coordinated iodide anion. The coordination of six potassium cations to the uranyl oxygen atoms had already been observed in the dbm tetramer $[UO_2(dbm)_2]_2[\mu\text{-}K(py)_2]_2[\mu_8\text{-}K(py)]_2I_2{\cdot}py_2$.

The two crystallographically independent U atoms in **2**, **3**, **4**, and **5** are seven-coordinated, with a slightly distorted pentagonal bipyramidal geometry, by two *trans* oxo groups, two nitrogen atoms, and two oxygen atoms from the Schiff base ligand and one bridging oxygen from the adjacent uranyl complex. For all complexes, the $UO_2^+\cdots UO_2^+$ interaction results in a significant lengthening of the U=O bond distance for the uranyl oxygen atoms involved in this interaction (U=O bond range 1.97–1.91 Å) with respect to the oxygen atoms that do not participate to the $UO_2^+\cdots UO_2^+$ (U=O bond range = 1.87–1.77 Å) with a similar mean difference between the two U=O bonds of about 0.1 Å.

The salophen and the acacen ligands adopt a so-called "boat" conformation,[53,54] whereas the salen coordination in all complexes is almost planar. The mean $U{-}N_{Schiff\ base}$ and $U{-}O_{Schiff\ base}$ bond lengths are very similar in the salen (mean U–N = 2.63(3) Å in **2**, mean U–O = 2.36(2) Å in **2**) and in the salophen (mean U–N = 2.64(3) Å in **5**; mean U–O = 2.34(3) Å in **5**) complexes. In the acacen complex **4**, the mean $U{-}N_{Schiff\ base}$ length (2.48(9) Å) is significantly shorter probably due to the higher flexibility of the ligand, whereas the mean U–O distance (= 2.36(1) Å) is in the range found for the other Schiff bases. In **3** the $U{-}N_{Schiff\ base}$ bond lengths are longer for the ligand adjacent to the coordinated $([18]C\text{-}6)K)^+$. The mean U–salophen distances in complex **5** are very close to those found in the mononuclear complex $[U^VO_2(salophen\text{-}t\mathrm{Bu}_2)(thf)]K$ ($U{-}N_{av} = 2.60(2)$; $U{-}O_{av} = 2.39(4)$ Å).[21]

The major difference between the tetrameric complexes **2**, **3**, **4**, and **5** is found in the metric parameter of the square core. Whereas the core geometry is very similar in the acacen and salen tetramers (mean value of the U–U distance = 4.30(6) in **4** and 4.31(3) Å in **2**; mean value of the U-O-U angle = 173.40(6) in **4** relative to 172.2(7)° in **2**), the metric parameters are significantly modified in **5**, with a shorter mean U–U distance (4.23(2) Å) and a smaller mean U-O-U angle (154.9(6)°; Figure 4). The shorter U–U distance can be related to the presence of two additional potassium ions bridging the uranyl groups in **5** with respect to the other complexes. As a result of the potassium coordination, the core geometry in **5** is significantly distorted from a square. The distortion of the core observed in **5** could play a role in the low stability of the pentavalent uranyl in this tetrameric cation–cation complex resulting in its rapid disproportionation. Moreover, the presence of a different number of potassium ions coordinated to the uranyl oxygen atoms in the salophen complex with respect to the salen and acacen analogues probably mirrors a difference in the charge at the uranyl oxygen atoms, which is likely to play a role in the observed differences of stability. Future work will be directed at investigating the electronic structure of these complexes.

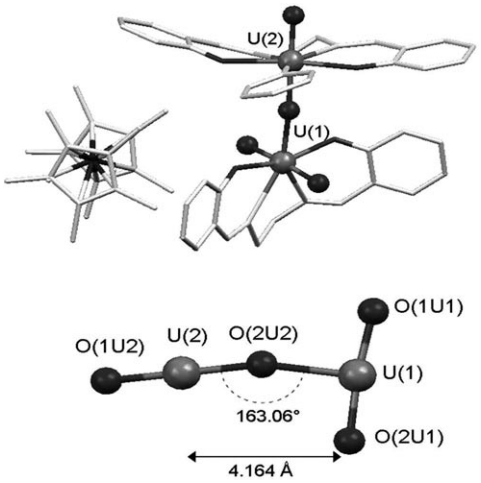

Figure 4. Mercury diagram of complex **8** and a detail of the T-shaped UO_2^{2+}–UO_2^+ interaction in **6** with associated distances and angles. (H atoms were omitted for clarity, ligands are represented with grey pipes, O in black, and U in grey. Disorder on one of the pentamethylcyclopentadiene groups has not been represented.) Selected bond lengths [Å] and angles [°]: U(1)–O(1U1): 1.792(12), U(1)–O(2U1): 1.801(12), U(1)–O(1): 2.268(13), U(1)–O(1U2): 2.277(10), U(1)–O(2): 2.283(11), U(1)–N(2): 2.581(15), U(1)–N(1): 2.627(15), U(2)–O(2U2): 1.820(13), U(2)–O(1U2): 1.933(10), U(2)–O(21): 2.318(12), U(2)–O(22): 2.317(13), U(2)–N(22): 2.596(13), U(2)–N(21): 2.620(14), U(2)–N(py): 2.666(13); O(1U1)-U(1)-O(2U1): 173.6(5), O(2U2)-U(2)-O(1U2): 179.0(6), U(2)-O(1U2)-U(1): 163.0(6).

Reactivity: To gain new insight into the parameters leading to stable cation–cation species of pentavalent uranyl complexes versus disproportionation intermediates we have performed reactivity studies on the tetrameric cation–cation complexes prepared in this work. Previous studies of the reactivity of the isolated tetrameric and dimeric cation–cation dbm complexes of pentavalent uranyl in different solvents had allowed the identification of $U^{VI}O_2^{2+}$ and U^{IV} species as disproportionation products, but the stoichiometry of the reaction remained ambiguous and the fate of the uranium and uranyl oxygen atoms was only partly identified.[27] The preliminary studies on the dbm complexes pointed to the implication of the cation–cation species in the disproportionation and to an important effect of the solvent and cation on the reactivity. The Schiff base complexes prepared here provide a great opportunity for gaining further insight into the disproportionation reaction. Notably, their stability renders it possible to study the effect of added protons and cations on the disproportionation mechanism. Moreover the higher denticity of the Schiff base ligands with respect to the previ-

ously investigated systems prevents ligand dissociation making the study of the decomposition products easier.

The salophen complex of pentavalent uranyl in pyridine in the presence of K^+ undergoes rapid disproportionation preventing the isolation of cation–cation intermediates. Similar to what was observed for the dbm complexes, many different disproportionation products are formed, which are difficult to characterize except for $[U(salophen)_2]$ and $[UO_2(salophen)S]$ derivatives, which were identified by ^1H NMR spectroscopy (see Figure S2 in the Supporting Information) and mass spectroscopy (ESI-MS peaks at m/z: 584.3 for $[UO_2(salophen)]^+$ and 866.3 for $[U(salophen)_2]^+$). The complexity of this reaction prevents the identification of the other products. Notably, in aprotic conditions a strong interaction can occur between the unreacted pentavalent complex and the reaction products affording new species and rendering even more complex the characterization of the final mixture. Such interactions were clearly identified for the salen derivatives. In a previous report we have shown that the treatment of a dark-blue solution of **2** in pyridine (0.75 equivalents of **2**) with one equivalent of $[U^{VI}O_2(salen)(py)]$ (**7**) yields the mixed-valent uranyl(VI)/uranyl(V) cation–cation complex, $\{[UO_2(salen)\mu\text{-}K(18C6)][UO_2(salen)]_3[\mu_8\text{-}K]_2\}$.[35] In this mixed-valent tetramer a strong CCI occurs between the uranyl(V) oxygen and the uranium ion of the uranyl(VI), as a result of the greater basicity of the UO_2^+ oxygen atoms with respect to the hexavalent analogue and of the Lewis acidity of the UO_2^{2+} ion. In line with this result, we have now investigated the reaction of $[U^{VI}O_2(salen)(py)]$ with $[U^{V}O_2(salen)(py)][Cp^*_2Co]$ in a 1:1 ratio (Scheme 3).[35] This reaction allows the preparation of the dinuclear mixed valent complex $[UO_2(salen)(py)]_2[Cp^*_2Co]$ (**8**), which can be isolated as a dark-green crystalline solid in 92% yield. The ^1H NMR spectrum of **8** differs from those of the starting materials and shows the presence of a new paramagnetic species. This dimeric complex is stable for up to one month in pyridine solution.

A Mercury diagram[55] of the crystal structure of the complex **8** is shown in Figure 4. The smaller values of the U=O bond lengths (1.792(12) and 1.801(12) Å) found for U1 with respect to the other uranyl group distances (1.820(13)–1.933(10) Å for U2) suggests that the valence is localized, with U(1) identified as U^{VI}. Very similar values of the U^{VI}=O bond lengths were found for the previously reported mixed-valent tetramer, $\{[UO_2(salen)\mu\text{-}K([18]C\text{-}6)][UO_2(salen)]_3[\mu_8\text{-}K]_2\}$,[35] and in extended frameworks presenting $UO_2^{2+}\cdots UO_2^{2+}$ cation–cation interactions.[56,57] Both uranium ions are heptacoordinated with a slightly distorted pentagonal bipyramid geometry by the four donor atoms of the salen ligand situated in the equatorial plane and the two uranyl oxygen atoms in an axial position; the seventh coordination position is occupied by a pyridine nitrogen atom in the U^V complex and by a uranyl oxygen atom from the UO_2^+ group in the U^{VI} complex. This dimeric complex provides a second example of an isolated molecular U^V/U^{VI} compound. Mixed-valent U^V/U^{VI} systems have been identified in a few naturally occurring oxide minerals[58] and in rare examples of oxide compounds obtained under hydrothermal conditions.[59–61] The first example of mixed-valent Np^V/Np^{VI} cation–cation complexes has also been recently isolated.[42] These results show that interactions can occur between U^V and the decomposition products rendering the assignment of all disproportionation products more difficult. The possible formation of U^V/U^{VI} species had been anticipated from kinetic studies on the disproportionation reaction of aqua pentavalent uranyl. The formation of these species was demonstrated to lead to a stabilization of the pentavalent uranyl complex in water.[62]

The observed difference in reactivity with respect to the disproportionation reaction between the salophen system and the salen tetramer is quite remarkable considering the similarity of these two ligands. Previous DFT studies on mononuclear pentavalent uranyl complexes of salen and salophen ligands had suggested the presence of a similar electronic structure and stability for the two systems.[63] In the absence of coordinating cations or in solvent conditions (DMSO) for which the potassium cation does not coordinate to the uranyl oxygen atom, the resulting monomeric complexes $[UO_2(salophen)(py)][Cp^*_2Co]$ (**6**) and $[UO_2(salophen)(dmso)]^-$[24] are stable with respect to the disproportionation reaction, which is similar to what was found for the salen derivatives. The results presented here suggest that the cation–cation interaction is favored for these complexes by the presence of the coordinating cation and that the stability of the resulting polynuclear complex is

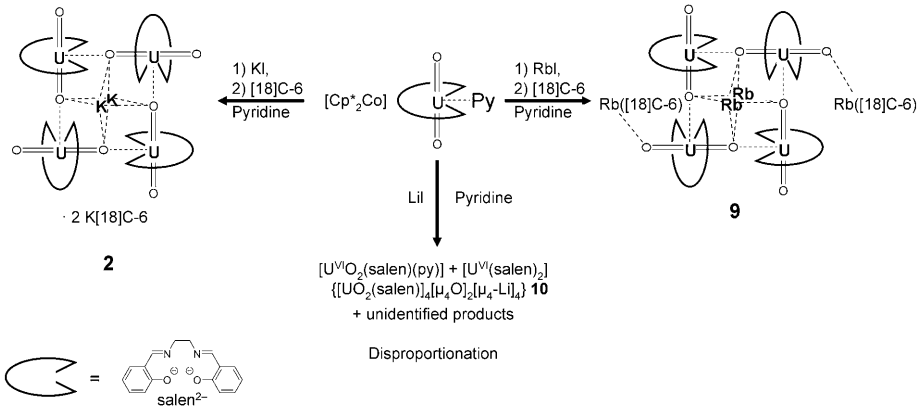

Scheme 3. Reaction of the complex $[UO_2(salen)(py)][Cp^*_2Co]$ with different alkali cations showing the effect of the cation on the stability of the U^V complex.

different in the two ligand systems. The potassium cation has two different roles in these complexes. The structural role of potassium leading to tetramer formation has been clearly identified in this and previous work.[27,35] Potassium has also an electronic effect, notably it stabilizes the pentavalent uranyl species with respect to the oxidation reaction by decreasing the negative charge on the uranyl oxygen atom.[21] We have also observed that replacing K^+ with $K([18]C\text{-}6)^+$ is sufficient to stabilize the salophen tetramer against disproportionation. To gain further insight on the differences in reactivity between salen and salophen and on the effect of counterions we have studied the reactivity of the monomeric complex $[UO_2(salen)(py)][Cp^*_2Co]$ with different alkali ions. The reaction of $[UO_2(salen)(py)][Cp^*_2Co]$ with KI and RbI results in the formation of the tetrameric complexes **2** and $\{[UO_2(salen)_4][\mu_8\text{-}Rb]_2[Rb([18]C\text{-}6)]_2\}$ (**9**), respectively (Scheme 3).

The two complexes show very similar structures and they both have a high stability in pyridine with respect to the disproportionation reaction. However, some structural differences are observed in **9** with respect to **2** as a result of the larger size of the Rb^+ cation (Figure 5). The mean values of the $Rb{-}O_{yl}$ and of the $Rb{-}O_{salen}$ bond lengths (3.17(16) and 2.83(4) Å) are longer than the respective $K{-}O_{yl}$ and $K{-}O_{salen}$ bond lengths (2.99(18) and 2.70(4) Å). This results in a shorter distance between the oxygen atoms of adjacent salen ligands for **2** and a shorter distance between the potassium cation and the mean plane defined by the four uranium centers (K-mean plane distance = 2.14 Å in **2** and Rb-mean plane distance = 2.37 Å in **9**), leading to a slightly increased distortion from planarity of the salen ligand in the Rb complex.

The presence of a different cation does not result in a different reactivity and both **2** and **9** are stable in pyridine with respect to the disproportionation reaction. In contrast, the reaction of $[UO_2(salen)(py)][Cp^*_2Co]$ with the iodide salt of the smaller Li^+ ion results in the slow disproportionation of the resulting pentavalent complex yielding a mixture of decomposition products (Scheme 3). The ^1H NMR spectrum of the reaction mixture recorded after 30 days shows the presence of the $[U(salen)_2]$ complex and of a $[U^{VI}O_2(salen)(py)]$ (**7**) species and an additional unidentified species (see Figure S6 in the Supporting Information). This difference in reactivity with respect to the rubidium and potassium complexes could result from the very small size of the Li^+ ion, which probably promotes the formation of cation–cation complexes with a lower stability. The lower stability of the UO_2^+ complex of salen in the presence of Li^+ is probably the result of both sterical and electronic effects associated to the higher ratio charge/ionic radii of Li^+ relative to K^+ and Rb^+. From the decomposition mixture, we were able to isolate crystals of an interesting decomposition product. X-ray diffraction shows the presence of the oxo uranyl cluster $\{[UO_2(salen)]_4[\mu_4\text{-}O]_2[\mu_4\text{-}Li]_4\}$ (**10**). A Mercury diagram of the structure of **10** is presented in Figure 6. The quality of the structure is not sufficient for a discussion of the bond distances or for the localization of the solvents molecules. It is therefore difficult to unambiguously assign the uranium ions oxidation state in the complex. However the connectivity of the structure is unambiguous. The structure consists of four uranyl groups arranged in a tetrahedral geometry. The uranyl groups are connected by two oxo groups bridging two adjacent U ions and by four Li^+ ions yielding a $[U_4Li_4]$ cubic cluster. Each Li ion is quadruply bridged to two salen oxygen atoms, one uranyl oxygen atom, and one bridging

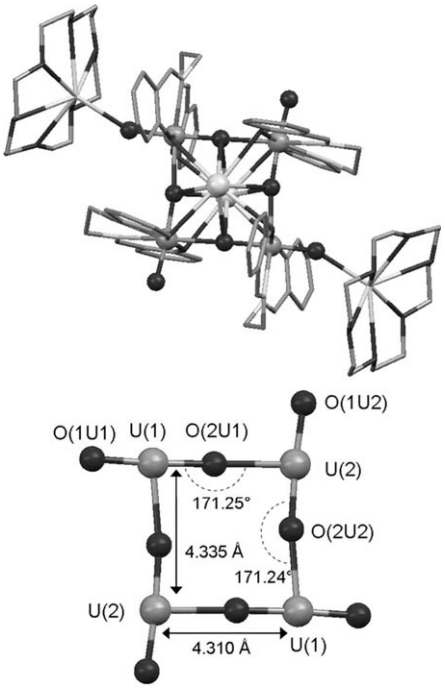

Figure 5. Mercury view of the structure of **9** (left) and detail of the core with associated distances and angles (right). The structures are represented along the axis formed by the two rubidium ions perpendicular to the uranium square plane (for clarity H atoms were omitted and only one of the two positions of the disordered Rb([18]C-6) group is shown; ligands are represented with grey pipes, O in black, Rb in white, and U in grey.).

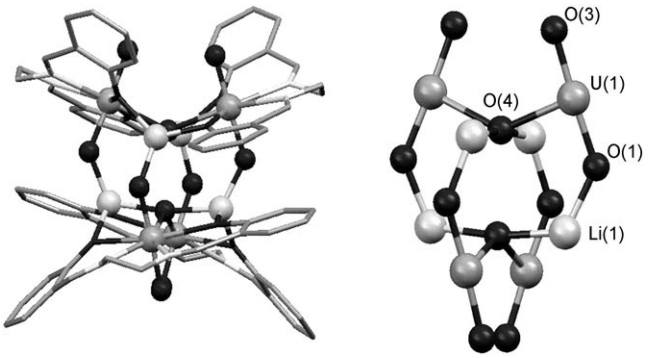

Figure 6. Mercury view and core detail of complex **10**. (H atoms were omitted for clarity; ligands are represented with grey pipes, O in black, Li in white, and U in grey.)

oxo-group. The presence of the μ-oxo groups in the structure accounts for the fate of the oxygen atom in the disproportionation reaction of pentavalent uranyl compounds in aprotic solvents. While the formation of U^{IV} and U^{VI} species had already been unambiguously identified by ^{1}H NMR spectroscopic studies of the decomposition process of UO_2^+ dbm complexes, in the previous studies the fate of the oxygen remained unknown. The isolation of the decomposition product **10** demonstrates why it can be challenging to identify all the products of disproportionation of pentavalent uranyl in aprotic conditions.

The mechanism proposed from the DFT studies of the disproportionation of pentavalent uranyl in aqueous conditions involves the protonation of a cation–cation intermediate followed by electron transfer to yield the U^{IV} and U^{VI} aqua species and water.[18] The cation–cation complex **2** is stable in pyridine and can, therefore, be used to investigate the reactivity of cation–cation complexes with a stoichiometric amount of protons to demonstrate the important role of protons in the disproportionation of pentavalent uranyl. Notably, the addition of one equivalent of pyridinium chloride (per uranium center) to a solution of **2** resulted in the immediate disproportionation of the complex. The ^{1}H NMR spectrum of the decomposition products show a mixture of $[U^{VI}O_2(salen)(py)]$ (**7**) and of the uranium(IV) complexes $[U(salen)_2]$ and $[UCl_2(salen)]$, in a ratio of 6:2:3 (Scheme 4).

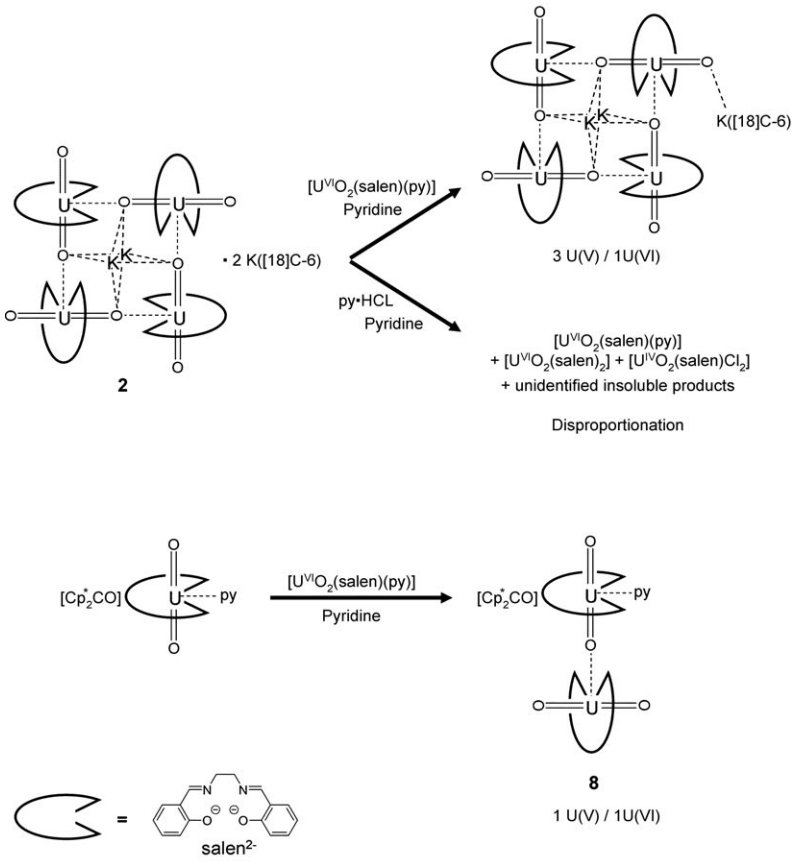

Scheme 4. Reaction of the pentavalent complexes of salen with hexavalent uranyl or protons leading to oxo-group functionalization and to disproportionation, respectively.

All these products were characterized by ^{1}H NMR spectroscopy and single-crystal X-ray diffraction for **7**.[52] The formation of water in this reaction was characterized by ^{1}H NMR spectroscopy (Figure 7). The stoichiometry of the reaction suggests that additional U^{IV} species must form during decomposition. The reaction presented here is in perfect agreement with the mechanism proposed from theoretical studies for the disproportionation of pentavalent uranyl in water.[8,18] This reactivity highlights the important role played by the protons in the mechanism of disproportionation and confirms that the protonation of one oxygen atom to form a better leaving group is a key step in the disproportionation mechanism. In the absence of protons, stable cation–cation complexes can form depending on the ligand and reaction conditions. However for some ligand systems (such as salophen and dbm) the disproportionation occurs also in aprotic solvents, but leads to the formation of more complex species and probably follows a different pathway.

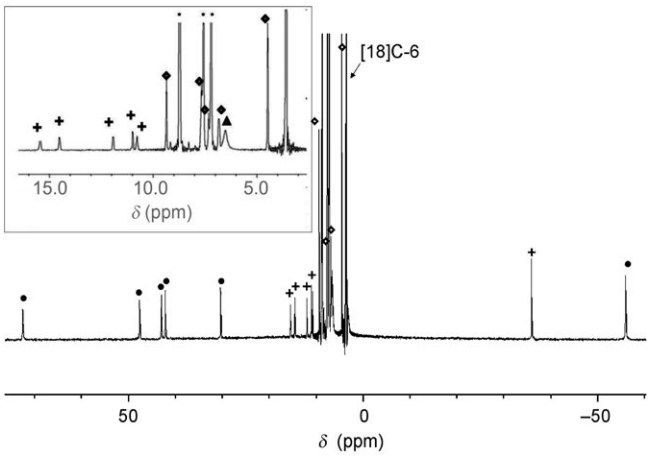

Figure 7. ^{1}H NMR spectrum of **2** in pyridine after the addition of py•HCl. ●: $U^{IV}Cl_2(salen)$; +: $U^{IV}(salen)$; ◆: $U^{VI}O_2(salen)$; *: pyridine; ▲: water.

Conclusion

In this work two new stable cation–cation complexes of pentavalent uranyl have been prepared by using the Schiff base ligands acacen and salophen. The results presented here show that in contrast with what was previously postulated, the cation–cation interaction does not necessarily lead to disproportionation in a nonprotic media. Conversely, highly stable polynuclear complexes can be obtained, but a careful tuning of the ligand geometry and electronic properties is required. Moreover, the presence of the coordinating counterions is essential in the formation of polymetallic structure and the nature of the cation has a crucial effect on their stability with respect to the disproportionation reaction. The isolated species are stable even in the presence of stoichiometric amounts of water. In contrast, the reaction of these stable tetrameric complexes with H^+ leads to the immediate disproportionation of the cation–cation complexes and to the formation of mononuclear UO_2^{2+} and U^{IV} species and H_2O. Depending on the electronic and geometric properties of the chosen Schiff base and on the reaction conditions (solvent, type of coordinating cation) the disproportionation occurs also in nonprotic solvents but leads to different decomposition products. The isolation of an oxo–uranyl cluster as a decomposition product shows that in nonprotic anaerobic conditions the disproportionation reaction leads to complex polyoxo clusters rather than to the anticipated formation of mononuclear UO_2^{2+} and U^{IV} species. These results provide important information on the key role played by cation–cation interactions and protons in the mechanism of disproportionation of pentavalent uranyl. Moreover, the presented results show that the interaction between pentavalent uranyl compounds provides an excellent route for the formation of polynuclear complexes of uranium presenting different electronic and geometric structure. The nature of the cation appears to be the key to the preparation of stable polynuclear complexes of uranyl(V) with different ligands. Work in this direction is in progress.

Experimental Section

General considerations: All manipulations were carried out under an inert argon atmosphere by using Schlenk techniques and an MBraun glovebox equipped with a purifier unit. The water and oxygen level were always kept at less than 1 ppm. The solvents were purchased from Aldrich in their anhydrous form conditioned under argon and were vacuum distilled from K/benzophenone (diisopropyl ether, hexane, pyridine and thf) or CaH_2 (acetonitrile). Depleted uranium turnings were purchased from the "Société Industrielle du Combustible Nucléaire" of Annecy (France). [18]Crown-6 ether and [2,2,2]cryptand were purchased from Aldrich and sublimated prior to use. The salen, salophen, and acacen ligands and their potassium salts were prepared as previously described.[64] $[UI_3(thf)_4]$,[30] $[(UO_2py_5)(KI_2py_2)]$,[28] $\{[UO_2(salen)]_4[\mu_8\text{-}K]_2\}\cdot 2[K([18]C\text{-}6)(py)]$ (**2**), $[UO_2(salophen)(S)]$,[24] $[UO_2(salen)(S)]$ (S = py, thf) (**7**), and $[UO_2(salen)(py)][Cp^*_2Co]$[35] were synthesized as previously described. UV/Vis-NIR measurements were carried out with a Varian Cary 50 Probe spectrophotometer in quartz cells (optical path lengths: 1 mm) adapted with J. Young valves. Elemental analyses were performed under argon by the Analytische Laboratorien GMBH at Lindlar (Germany). Mass spectra were obtained with a Finnigan LCQ-ion trap equipped with an electrospray source in a pyridine/acetonitrile mixture 1:5, which was prepared and filtered on microporous filters in the glove-box and maintained under argon until injection in the spectrometer. The experimental isotopic profile was compared in each case to the theoretical one. ^{1}H NMR spectra were recorded on Varian MERCURY 400 and Bruker 200 and 500 MHz spectrometers. ^{1}H NMR spectroscopic chemical shifts are reported in ppm with solvent as an internal reference. ^{1}H NMR spectroscopic experiments were carried out by using a NMR tube adapted with J. Young valves.

Syntheses

$\{[UO_2(acacen)]_4[\mu_8\text{-}K]_2[K([18]C\text{-}6)(py)]_2\}$ (3): $[(UO_2py_5)(KI_2py_2)]_n$ (70 mg, 0.062 mmol) was added to a suspension of acacenK_2 (18.8 mg, 0.062 mmol, 1 equiv) in pyridine (2 mL), which resulted in a dark-red solution with a small amount of an off-white precipitate. After 1 h stirring at room temperature, the reaction mixture was filtered and [18]C-6 (34 mg, 0.124 mmol, 2.0 equiv) was added to the resulting solution. After 48 h stirring at room temperature, the solution color turned to pink. Slow diffusion of diisopropyl ether (6 mL) into this solution yielded after 2 days 15 mg of X-ray quality deep-red crystals of the tetrameric $\{[UO_2(acacen)]_4[\mu_8\text{-}K]_2[K([18]C\text{-}6)(py)]_2\}$complex (0.0054 mmol, 34%; the crystallization was stopped at a early stage to avoid the co-crystallization of K([18]C-6)I*, which explains the low yield of the reaction). These crystals are not very stable and easily loose the two pyridine molecules present in the unit cell when they were dried under vacuum for the elemental analysis. Elemental analysis calcd (%) for $\{[UO_2(acacen)]_4[\mu_8\text{-}K]_2[K([18]C\text{-}6)]_2\}$ ($C_{72}H_{120}N_8O_{28}K_4U_4$, M_r = 2654.29): C 32.58, H 4.56, N 4.22; found: C 32.47, H 4.77, N 4.53. ^{1}H NMR (no changes observed over 30 days; [D$_5$]pyridine; 298 K; 200 MHz): δ = −3.83 (s, 3H; $-CH_3$), −3.22 (s, 3H; $-CH_3$), 0.26 (br s, 1H; $-NCH_2-$), 1.09 (d, 2H; C−HC=C−), 3.80 (s, 24H; [18]C-6)*; higher yields (82%) can be obtained with a longer crystallization time (10 days), but the final compound presents two co-crystallized K([18]C-6)I; elemental analysis calcd (%) for $\{[UO_2(acacen)]_4[\mu_8\text{-}K]_2[K([18]C\text{-}6)]_2\}\cdot 2[K([18]C\text{-}6)I]$ ($C_{96}H_{168}N_8O_{40}K_4U_4$, M_r = 2654.29): C 32.80, H 4.82, N 3.19; found: C 32.79, H 4.61, N 3.39.

$\{[UO_2(acacen)]_4[\mu_8\text{-}K]\}\cdot 2[K([222])(py)]$ (4): $[(UO_2py_5)(KI_2py_2)]_n$ (50 mg, 0.044 mmol, 1 equiv) was added to a suspension of acacenK_2 (13.5 mg, 0.044 mmol, 1 equiv) in pyridine (2 mL), resulting in a dark-red solution with a small amount of an off-white precipitate. After 1 h stirring at room temperature, the reaction mixture was filtered and [2,2,2]cryptand (50.6 mg, 0.134 mmol, 3 equiv) was added to the resulting solution. After 2 h stirring at room temperature, the solution color turns to clear brown. Slow diffusion of diisopropyl ether (7 mL) into this solution yielded X-ray quality deep-red crystals of the tetrameric $[UO_2(acacen)]_4[\mu_8\text{-}K]\cdot 2[K([222])(py)]$ complex (17.8 mg, 0.0058 mmol, 53%). These crystals are not very stable and partially lost the pyridine molecules present in the unit cell when they were dried under vacuum for the elemental analysis. Elemental analysis calcd (%) for $[UO_2(acacen)]_4[\mu_8\text{-}K]\cdot 2[K([222])]\cdot 1.7$ py ($C_{92.5}H_{1552.5}N_{13.7}O_{28}K_4U_4$, M_r = 3013.14): C 36.87, H 5.10, N 6.37; found: C 36.84, H 4.92, N 5.98; ^{1}H NMR (no changes observed over 30 days; [D$_5$]pyridine; 298 K; 500 MHz): δ = −3.75 (s, 3H; $-CH_3$), −3.22 (s, 3H; $-CH_3$), 0.46 (br s, 1H; $-NCH_2-$); 1.16 (s, 1H; C−HC=C−), 2.38, 3.39, 3.44 (s, [2,2,2]cryptand), 6.80 (s, 1H; $-NCH_2-$); ESI-MS: 1023.2 [M^{2+}], 2046.9 [M^+].

$\{[UO_2(salophen)]_4[\mu_8\text{-}K]_2[\mu_5\text{-}KI]_2[(K([18]C\text{-}6)]\}\cdot 2[K([18]C\text{-}6)(thf)_2]\cdot 2I$ (5): A solution of salophenK_2 (36.0 mg, 0.090 mmol, 1 equiv) and [18]C-6 (78.1 mg, 0.296 mmol) in pyridine (3.0 mL) was added to $[(UO_2py_5)(KI_2py_2)]_n$ (100.0 mg, 0.090 mmol, 1 equiv), resulting instantly in a clear-green solution. The solution was stirred for 2 h and then filtered. The filtrate was concentrated under vacuum (0.5 mL). Addition of iPr$_2$O (7 mL) to the resulting solution yielded a green oil that was filtered, triturated in iPr$_2$O (5×3 mL), and dried under vacuum to yield a light-green powder (125.0 mg). This powder was recrystallized from THF (10 mL) to yield the title compound as dark-blue crystals (73 mg, 0.011 mmol, 51%). The compound co-crystallized with K([18]C-6)I, which could not be separated by further recrystallization. Elemental analysis calcd (%) for $[UO_2(salophen)]_4[\mu_8\text{-}K]_2[\mu_5\text{-}KI]_2[(K([18]C\text{-}6)]\cdot 2[K([18]C\text{-}6)(thf)_2]I$ ($C_{208}H_{312}I_9K_{13}N_8O_{75}U_4$, M_r = 6727.32): C 37.14, H 4.67, N 1.67, I 16.98;

found: C 36.84, H 4.92, N 2.06, I 17.28; ^{1}H NMR spectra of the green powder ([D$_5$]pyridine; 298 K; 400 MHz,): $\delta = 0.69$ (brd, 1H), 2.06 (brs, 1H); 3.86 (s, [18]C-6) 4.65 (brd, 1H), 4.78 (brt, 1H), 6.04 (brs, 1H), 6.26 (s, 1H), 7.01 ppm (brt, 1H).

[UO$_2$(salophen)(py)][Cp*$_2$Co] (6): Complex **6** was prepared in situ by following the procedure previously described for the complex [U^{V}O$_2$(salen)(py)][Cp*$_2$Co].[36] A bright-orange solution of [UO$_2$(salophen)(thf)] (5.0 mg, 0.008 mmol, 1 equiv) in [D$_5$]py (0.5 mL) was added to a suspension of Cp*$_2$Co (2.5 mg, 0.007 mmol, 1 equiv) in [D$_5$]py (0.5 mL), which resulted in a fast color change to deep green. The solution was stirred overnight at room temperature. The ^{1}H NMR spectrum of the resulting dark-green solution revealed the presence of an uranyl(V) complex of salophen. ^{1}H NMR ([D$_5$]pyridine; 298 K; 200 MHz, no changes observed over 15 days): $\delta = 0.35$ (brd, 1H), 1.53 (brs, 1H); 4.57 (brd, 1H), 4.62 (brt, 1H); 5.78 (s, 1H); 5.88 (brs, 1H); 7.03 (brt, 1H), 8.38 (brs, around 20H; Cp*$_2$Co$^+$/Cp*$_2$Co); this complex is stable in pyridine but its isolation was prevented by its lower stability after the addition of nonsolvents (necessary for the crystallization), such as *n*-hexane.

[UO$_2$(salen)(py)]$_2$·[Cp*$_2$Co] (8): Cp*$_2$Co (6.5 mg, 0.0195 mmol, 1 equiv) was added to a solution of [UO$_2$(salen)(thf)] (10.8 mg, 0.0395 mmol, 2 equiv) in py (1 mL) and the resulting suspension was stirred for 3 h. The solution became dark green after few minutes and did not change further with time. The solution was filtered and *n*-hexane was layered on the top of the filtrate (4 mL) to afford after 2 days green crystals (12 mg, 0.0081 mmol, 92%). Elemental analysis calcd (%) for [UO$_2$(salen)(py)]$_2$·[Cp*$_2$Co] ($C_{57}H_{63}N_5O_8CoU_2$, $M_r = 1481.15$): C 46.22, H 4.29, N 4.73; found: C 46.16, H 4.33, N 4.89; ^{1}H NMR ([D$_5$]pyridine; 298 K; 500 MHz,): $\delta = -3.36$ (brs, 1H), -0.24 (brs, 1H); 1.86 (brs, 30H; Cp*$_2$Co$^+$), 3.68 (s, 1H); 5.83 (s, 1H); 6.25 (s, 4H); 6.61 (s, 1H), 6.74 (brs, 1H), 7.69 (d, 1H), 8.10 (s, 1H), 10.62 (s, 1H), 11.99 ppm (s, 1H).

[UO$_2$(salen)$_4$][μ$_8$-Rb]$_2$[Rb([18]C-6)]$_2$ (9): Cp*$_2$Co (2.9 mg, 0.0088 mmol, 1 equiv) was added to a solution of [UO$_2$(salen)(thf)] (5.4 mg, 0.0088 mmol, 1 equiv) in pyridine (1 mL) and the resulting suspension was stirred for 6 h. The solution became dark green after few minutes and did not change further with time. RbI (1.9 mg, 0.0088 mmol) was added to this dark green solution, resulting in the immediate precipitation of a violet powder. This suspension was stirred for 3 h at room temperature, and then the violet precipitate was filtered and washed twice with pyridine (1 mL). A solution of [18]C-6 in pyridine (2.4 mg, 1 mL) was added to the resulting solid, to yield, after 16 h stirring at room temperature, a dark-blue solution. The solution was filtered and the filtrate was layered with *n*-hexane (2 mL) to yield after 2 days dark-violet crystals (3.6 mg) suitable for X-ray crystallography. The ^{1}H NMR spectrum ([D$_5$]pyridine; 298 K; 500 MHz) is identical to the that of **2**.

Reaction of 1 with salophenK$_2$: A solution of salophenK$_2$ (5.5 mg, 1 equiv) in pyridine (0.8 mL) was added to [(UO$_2$py$_5$)(KI$_2$py$_2$)]$_n$ (15.0 mg) at room temperature. The reaction mixture became yellow/green and was transferred to an NMR tube after 10 min. The ^{1}H NMR spectra (see Figure S2 in the Supporting Information) is complex, but the signals of [U(salophen)$_2$] and [UO$_2$(salophen)(S)] were already detected after 10 min and the chemical shifts are in good agreement with the ^{1}H NMR spectrum of separately synthesized compounds.

Reaction of 2 with py·HCl: A solution of py·HCl (1.4 mg, 0.012 mmol, 4 equiv) in [D$_5$]pyridine (0.5 mL), was added to a solution of **2** (7.5 mg, 0.003 mmol, 1 equiv) in [D$_5$]pyridine (2 mL) resulting in an immediate color change of the solution, from dark blue to yellow. The ^{1}H NMR spectrum of this solution clearly indicated the presence of three species, [UO$_2$(salen)(py)], [U(salen)$_2$], and [UCl$_2$(salen)], identified by comparison with the separately synthesized complexes.[52] The presence of water as a reaction product was clearly identified by ^{1}H NMR spectroscopy.

Reaction of {[UO$_2$(salen)][Cp*$_2$Co]} with LiI: [UO$_2$(salen)][Cp*$_2$Co] was prepared "in situ" by the addition of Cp*$_2$Co (5.7 mg, 0.017 mmol, 1 equiv) to a solution of [UO$_2$(salen)(thf)] (10.4 mg, 0.017 mmol, 1 equiv) in pyridine (1 mL). LiI (2.3 mg, 0.017 mmol, 1 equiv) was added to the resulting dark-green solution. The addition leads to an immediate color change to dark red. The solution was stirred another 72 h and then filtered. Slow diffusion of *i*Pr$_2$O (3 mL) affords after 7 days red/brown crystals of {[UO$_2$(salen)]$_4$[μ$_4$-O]$_2$[μ$_4$-Li]$_4$} (**10**) as well as a significant quantity of intractable red precipitate.

X-ray crystallography: Diffraction data were taken by using an Oxford-Diffraction XCallibur S kappa geometry diffractometer ($Mo_{K\alpha}$ radiation, graphite monochromator, $\lambda = 0.71073$ Å). To prevent evaporation of co-crystallized solvent molecules, the crystals were coated with light hydrocarbon oil and the data were collected at 150 K. The cell parameters

Table 2. X-ray crystallographic data for complexes **3**–**5** and **8**–**10**.

	3	**4**	**5**	**8**	**9**	**10**
formula	$C_{77}H_{125}K_4N_9O_{28}U_4$	$C_{94}H_{154}K_4N_{14}O_{28}U_4$	$C_{148}H_{192}I_4K_8N_8O_{45}U_4$	$C_{57}H_{63}CoN_5O_8U_2$	$C_{127.88}H_{144.10}N_{16.11}O_{28}Rb_4U_4$	$C_{64}H_{56}Li_4N_8O_{18}U_4$
crystal size [mm]	0.19×0.12×0.06	0.07x 0.04×0.04	0.25×0.10×0.05	0.40×0.22×0.04	0.29×0.10×0.08	0.11×0.08×0.05
crystal system	triclinic	triclinic	monoclinic	triclinic	triclinic	orthorhombic
space group	$P\bar{1}$	$P\bar{1}$	$P21/c$	$P\bar{1}$	$P\bar{1}$	$Fddd$
V [Å^3]	2529.4(3)	2938.66(19)	8536.3(3)	2657.4(2)	3354.5(2)	16463(2)
a [Å]	12.4344(6)	11.4327(4)	20.5597(4)	11.9294(6)	14.6577(7)	13.6929(17)
b [Å]	14.8771(10)	15.8095(6)	18.7475(4)	14.3569(8)	14.9748(6)	34.252(2)
c [Å]	15.0363(10)	17.1320(6)	22.2997(5)	17.4038(10)	18.4509(7)	35.101(2)
α [°]	90.871(5)	72.969(3)	90	67.132(5)	102.435(3)	90
β [°]	110.338(5)	83.061(3)	96.718(2)	76.897(4)	95.307(3)	90
γ [°]	102.879(5)	87.080(3)	90	78.995(4)	119.302(4)	90
Z	1	1	4	2	1	8
F_w [g mol^{-1}]	2733.38	3036.83	4575.62	1481.11	3648.77	2205.05
ρ [g cm^{-3}]	1.794	1.716	1.780	1.851	1.806	1.779
absorption coefficient [mm^{-1}]	6.620	5.709	4.779	6.447	6.331	7.907
F(000)	1318	1484	4456	1430	1764	8160
T [K]	150.0(2)	150.0(2)	150.0(2)	150.0(2)	150(2)	150(2)
total no. reflections	24310	22978	103664	31133	41616	9893
unique reflections [R-(int)]	8448 [0.0777]	9995 [0.0714]	32220 [0.0463]	10468 [0.0693]	11391 [0.0641]	2549 [0.0466]
final R indices [$I > 2\sigma(I)$]	$R1 = 0.0717$, $wR2 = 0.1739$	$R1 = 0.0592$, $wR2 = 0.1000$	$R1 = 0.0466$, $wR2 = 0.0992$	$R1 = 0.0992$, $wR2 = 0.2483$	$R1 = 0.1010$, $wR2 = 0.2985$	$R1 = 0.0814$, $wR2 = 0.2145$
largest diff. peak and hole [e A^{-3}]	4.567, −1.215	1.946, −0.852	3.522, −0.810	10.592, −1.674	7.862, −2.395	2.103, −0.713
GOF	0.876	0.735	0.747	1.050	1.042	0.971

were obtained with intensities detected on three batches of five frames. The crystal-detector distance was 4.5 cm. The number of settings and frames has been established by taking into consideration the laue symmetry of the cell by CrysAlisPro Oxford-diffraction software (for **3**), 271 (for **4**), 451 (for **5**), 803 (for **8**), 737 (for **9**), and 179 (for **10**) narrow data were collected for 1° increments in ω with a 60 s exposure time for **3**, 20 s for **4**, 30 s for **5**, 5 s for the first 192 frames of **8**, and 40 s for the other ones, 30 s for **9**, and 30 s for the first 58 frames of **10** and 140 s for the other ones. Unique intensities detected on all frames by using the Oxford-diffraction Red program were used to refine the values of the cell parameters. The substantial redundancy in data allows empirical absorption corrections to be applied by using multiple measurements of equivalent reflections with the ABSPACK Oxford-diffraction program. Space groups were determined from systematic absences, and they were confirmed by the successful solution of the structure. The structures were solved by direct methods by using the SHELXTL 6.14 package and for all structures all atoms, including hydrogen atoms, were found by difference Fourier syntheses. All non-hydrogen atoms were anisotropically refined on F^2 in **3**, **4**, **5**, **8**, **9**, and **10**. Hydrogen atoms were fixed in ideal position. Experimental details for X-ray data collections of all complexes are given in Table 2. CCDC-781955–781960 (for complexes **3**–**5** and **8**–**10**) contain the supplementary crystallographic data for this paper. These data can be obtained free of charge from The Cambridge Crystallographic Data Centre via www.ccdc.cam.ac.uk/data_request/cif. Color versions of Figures 3–6 representing the Mercury diagram of the structures can be found in the Supporting Information.

Acknowledgements

We thank P.-A. Bayle for his help with the NMR spectroscopic measurements and C. Lebrun for recording mass spectra.

[1] L. R. Morss, N. M. Edelstein, J. Fuger, *The Chemistry of the Actinide and Transactinide Elements*, Springer, Dordrecht, **2006**.
[2] E. S. Ilton, A. Haiduc, C. L. Cahill, A. R. Felmy, *Inorg. Chem.* **2005**, *44*, 2986–2988.
[3] Y. Suzuki, S. D. Kelly, K. M. Kemner, J. F. Banfield, *Nature* **2002**, *419*, 134.
[4] B. H. Gu, H. Yan, P. Zhou, D. B. Watson, M. Park, J. Istok, *Environ. Sci. Technol.* **2005**, *39*, 5268–5275.
[5] J. C. Renshaw, L. J. C. Butchins, F. R. Livens, I. May, J. M. Charnock, J. R. Lloyd, *Environ. Sci. Technol.* **2005**, *39*, 5657–5660.
[6] W. Luo, B. Gu, *Environ. Sci. Technol.* **2009**, *43*, 152–156.
[7] D. R. Lovley, E. J. P. Phillips, Y. A. Gorby, E. R. Landa, *Nature* **1991**, *350*, 413–416.
[8] M. Sundararajan, A. J. Campbell, I. H. Hillier, *J. Phys. Chem. A* **2008**, *112*, 4451–4457.
[9] A. Ikeda, C. Hennig, S. Tsushima, K. Takao, Y. Ikeda, A. C. Scheinost, G. Bernhard, *Inorg. Chem.* **2007**, *46*, 4212–4219.
[10] T. I. Docrat, J. F. W. Mosselmans, J. M. Charnock, M. W. Whiteley, D. Collison, F. R. Livens, C. Jones, M. J. Edmiston, *Inorg. Chem.* **1999**, *38*, 1879–1882.
[11] D. L. Clark, D. E. Hobart, M. P. Neu, *Chem. Rev.* **1995**, *95*, 25–48.
[12] C. R. Graves, J. L. Kiplinger, *Chem. Commun.* **2009**, 3831–3853.
[13] P. L. Arnold, J. B. Love, D. Patel, *Coord. Chem. Rev.* **2009**, *253*, 1973–1978.
[14] S. Fortier, T. W. Hayton, *Coord. Chem. Rev.* **2010**, *254*, 197–214.
[15] W. J. Evans, S. A. Kozimor, *Coord. Chem. Rev.* **2006**, *250*, 911–935.
[16] I. Castro-Rodríguez, K. Meyer, *Chem. Commun.* **2006**, 1353–1368.
[17] S. C. Bart, K. Meyer, *Struc. Bond.* **2008**, *127*, 119–176.
[18] H. Steele, R. J. Taylor, *Inorg. Chem.* **2007**, *46*, 6311–6318.
[19] A. Ekstrom, *Inorg. Chem.* **1974**, *13*, 2237–2241.
[20] K. Takao, M. Kato, S. Takao, A. Nagasawa, G. Bernhard, C. Hennig, Y. Ikeda, *Inorg. Chem.* **2010**, *49*, 2349.
[21] G. Nocton, P. Horeglad, V. Vetere, J. Pecaut, L. Dubois, P. Maldivi, N. M. Edelstein, M. Mazzanti, *J. Am. Chem. Soc.* **2010**, *132*, 495.
[22] C. Miyake, T. Kondo, S. Imoto, H. Ohyanishiguchi, *J. Less-Common Met.* **1986**, *122*, 313–317.
[23] K. Mizuoka, S. Tsushima, M. Hasegawa, T. Hoshi, Y. Ikeda, *Inorg. Chem.* **2005**, *44*, 6211–6218.
[24] K. Mizuoka, S. Y. Kim, M. Hasegawa, T. Hoshi, G. Uchiyama, Y. Ikeda, *Inorg. Chem.* **2003**, *42*, 1031–1038.
[25] K. Takao, S. Tsushima, S. Takao, A. C. Scheinost, G. Bernhard, Y. Ikeda, C. Hennig, *Inorg. Chem.* **2009**, *48*, 9602–9604.
[26] K. Mizuoka, Y. Ikeda, *Inorg. Chem.* **2003**, *42*, 3396–3398.
[27] G. Nocton, P. Horeglad, J. Pecaut, M. Mazzanti, *J. Am. Chem. Soc.* **2008**, *130*, 16633–16645.
[28] L. Natrajan, F. Burdet, J. Pecaut, M. Mazzanti, *J. Am. Chem. Soc.* **2006**, *128*, 7152–7153.
[29] F. Burdet, J. Pecaut, M. Mazzanti, *J. Am. Chem. Soc.* **2006**, *128*, 16512–16513.
[30] L. R. Avens, S. G. Bott, D. L. Clark, A. P. Sattelberger, J. G. Watkin, B. D. Zwick, *Inorg. Chem.* **1994**, *33*, 2248–2256.
[31] T. W. Hayton, G. Wu, *J. Am. Chem. Soc.* **2008**, *130*, 2005–2014.
[32] T. W. Hayton, G. Wu, *Inorg. Chem.* **2008**, *47*, 7415–7423.
[33] P. Horeglad, G. Nocton, Y. Filinchuck, J. Pécaut, M. Mazzanti, *Chem. Commun.* **2009**, 1843–1845.
[34] P. L. Arnold, D. Patel, C. Wilson, J. B. Love, *Nature* **2008**, *451*, 315–318.
[35] V. Mougel, P. Horeglad, G. Nocton, J. Pecaut, M. Mazzanti, *Angew. Chem.* **2009**, *121*, 8629–8632; *Angew. Chem. Int. Ed.* **2009**, *48*, 8477–8480.
[36] N. N. Krot, M. S. Grigoriev, *Russ. Chem. Rev.* **2004**, *73*, 89–100.
[37] P. M. Almond, S. Skanthakumar, L. Soderholm, P. C. Burns, *Chem. Mater.* **2007**, *19*, 280–285.
[38] T. Z. Forbes, P. C. Burns, S. Skanthakumar, L. Soderholm, *J. Am. Chem. Soc.* **2007**, *129*, 2760–2761.
[39] S. Skanthakumar, M. R. Antonio, L. Soderholm, *Inorg. Chem.* **2008**, *47*, 4591–4595.
[40] I. A. Charushnikova, N. N. Krot, Z. A. Starikova, *Radiochim. Acta* **2007**, *95*, 495–499.
[41] M. S. Grigoriev, N. N. Krot, A. A. Bessonov, K. Y. Suponitsky, *Acta Crystallogr. Sect. A* **2007**, *63*, M561–M652.
[42] S. M. Cornet, L. J. L. Haller, M. J. Sarsfield, D. Collison, M. Helliwell, I. May, N. Kaltsoyannis, *Chem. Commun.* **2009**, 917–919.
[43] I. Charushnikova, E. Bosse, D. Guillaumont, P. Moisy, *Inorg. Chem.* **2010**, *49*, 2077–2082.
[44] M. J. Sarsfield, R. J. Taylor, C. J. Maher, *Radiochim. Acta* **2007**, *95*, 677–682.
[45] W. J. Evans, S. A. Kozimor, J. W. Ziller, *Science* **2005**, *309*, 1835–1838.
[46] G. Nocton, J. Pecaut, M. Mazzanti, *Angew. Chem.* **2008**, *120*, 3082–3084; *Angew. Chem. Int. Ed.* **2008**, *47*, 3040–3042.
[47] J. L. Kiplinger, J. A. Pool, E. J. Schelter, J. D. Thompson, B. L. Scott, D. E. Morris, *Angew. Chem.* **2006**, *118*, 2090–2095; *Angew. Chem. Int. Ed.* **2006**, *45*, 2036–2041.
[48] Higher yields can be obtained, but they result in contamination of the final product with potassium salts.
[49] J. T. J. Edward, *Chem. Educ.* **1970**, *47*, 261–269.
[50] G. Bellachioma, G. Ciancaleoni, C. Zuccaccia, D. Zuccaccia, A. Macchioni, *Coord. Chem. Rev.* **2008**, *252*, 2224–2238.
[51] L. Allouche, A. Marquis, J.-M. Lehn, *Chem. Eur. J.* **2006**, *12*, 7520–7525.
[52] M. Mazzanti, V. Mougel, B. Biplab, unpublished results.
[53] G. Bandoli, D. A. Clemente, U. Croatto, M. Vidali, P. A. Vigato, *J. Chem. Soc. Dalton Trans.* **1973**, 2331–2335.
[54] B. Zarli, R. Graziani, E. Forselli, U. Croatto, G. Bombieri, *J. Chem. Soc. Chem. Commun.* **1971**, 1501–1502.
[55] C. F. Macrae, P. R. Edgington, P. McCabe, E. Pidcock, G. P. Shields, R. Taylor, M. Towler, J. van de Streek, *J. Appl. Crystallogr.* **2006**, *39*, 453–457.
[56] T. A. Sullens, R. A. Jensen, T. Y. Shvareva, T. E. Albrecht-Schmitt, *J. Am. Chem. Soc.* **2004**, *126*, 2676–2677.

[57] E. V. Alekseev, S. V. Krivovichev, W. Depmeier, O. I. Siidra, K. Knorr, E. V. Suleimanov, E. V. Chuprunov, *Angew. Chem.* **2006**, *118*, 7391–7393; *Angew. Chem. Int. Ed.* **2006**, *45*, 7233–7235.
[58] P. C. Burns, J. F. Finch, *Am. Mineral.* **1999**, *84*, 1456–1460.
[59] N. Belai, M. Frisch, E. S. Ilton, B. Ravel, C. L. Cahill, *Inorg. Chem.* **2008**, *47*, 10135–10140.
[60] F. C. Hawthorne, R. J. Finch, R. C. Ewing, *Can. Mineral.* **2006**, *44*, 1379–1385.
[61] C. H. Lin, K. H. Lii, *Angew. Chem.* **2008**, *120*, 8839–8841; *Angew. Chem. Int. Ed.* **2008**, *47*, 8711–8713.
[62] T. W. Newton, F. B. Baker, *Inorg. Chem.* **1965**, *4*, 1166–1170.
[63] V. Vetere, P. Maldivi, M. Mazzanti, *C. R. Chim.* **2010**, *13*, 876–883.
[64] M. Mazzanti, PhD thesis, Université de Lausanne (Switzerland), **1990**.

Received: July 8, 2010
Published online: November 4, 2010

